International Journal of Mass Spectrometry and Ion Physics, 24 (1977) 335—354

IN SITU CHEMICAL IONIZATION AS A PROBE FOR NEUTRAL CONSTITUENTS UPSTREAM IN A METHANE—OXYGEN FLAME

D.K. BOHME *, J.M. GOODINGS and CHUN-WAI NG

Department of Chemistry, York University, 4700 Keele Street, Downsview, Ontario M3J 1P3 (Canada)

(Received 10 November 1976)

ABSTRACT

The early stages of combustion are considered for a flame viewed as a site for in situ chemical ionization. This study explores the information provided by the measurement of axial concentration profiles for both positive and negative ion species upstream in a conical premixed methane—oxygen flame of fuel-lean composition (equivalence ratio = 0.2) burning at atmospheric pressure. Making use of existing energetic and kinetic data now available for individual ion—molecule reactions, the profile information can be interpreted to reveal the mechanisms which dominate the positive and the negative ion chemistry independently. Confidence in these general mechanisms leads in turn to interpretation of the nature and behaviour of the underlying neutral species present upstream in the flame. A neutral beam sampling study of a similar flame is available in the literature for comparison purposes, and our work corroborates the presence of a number of neutral species (O_2, H_2O, CO, CO_2, O, OH, HO_2, HCHO, CH_3OH, CH_3O_2). Initiated by the protons available from primary CHO^+ ions, the positive ion chemistry is dominated by fast proton transfer reactions which indicate the presence of other neutrals in protonated form (CH, CH_2, CH_3, C_2H_2, HCO, CH_3CHO, CH_2CO, CH_3CHCO and possibly C, HCOOH, C_2H_5CHO). The negative ion chemistry is more complicated, involving charge transfer, proton transfer and rearrangement with an uncertain contribution from three-body association reactions and switching reactions. Nevertheless, the negative ion data indicate the presence of several neutral species not previously reported for this fuel-lean flame (C_2H_2, CH_2CO, O_3 with inconclusive evidence for HCOOH).

INTRODUCTION

During the last decade, chemical ionization (CI) mass spectrometry has become established as a powerful technique for the analysis of a wide variety of sample compounds [1]. In the most general sense, the technique exploits the high efficiency and selectivity of several different types of ion—molecule reactions which can be used to ionize the sample. The ion chemistry proceeding in partially-ionized flames, although generally more complex than that occurring in a conventional CI source, can be viewed in a similar

* Alfred P. Sloan Research Fellow, 1974—76.

manner to provide information about the composition of the bath of neutral constituents in which the individual ion—molecule reactions proceed.

In this study we explore the information provided by measurement of axial concentration profiles for both positive- and negative-ion species upstream in a conical premixed methane—oxygen flame of fuel-lean composition (equivalence ratio $\phi = 0.2$) burning at atmospheric pressure. Good spatial resolution is obtained from the conical flame geometry which permits insertion of a sampling probe upstream. The individual ion profiles are interpreted to reflect the occurrence of chemical ionization processes which contain the required information about the neutral composition. The interpretation is based on a fairly complete understanding of the upstream ion chemistry made possible by recent studies of ion—molecule reactions in our own laboratories using the flowing afterglow technique [2] and elsewhere [3]. Molecular beam sampling studies of the predominant neutral species present in a low-pressure flame of similar fuel-lean composition are available for comparison purposes [4]. The primary aim of this research is to ascertain what can be learned about the early stages of combustion when a flame is viewed as a site for in situ chemical ionization.

EXPERIMENTAL

The premixed fuel-lean flame was burned vertically on a simple cylindrical quartz capillary burner (2.3-mm i.d.) with methane and oxygen flow rates of 1.76 and 16.3 atmospheric $cm^3\ s^{-1}$, respectively. The luminous reaction zone was about 0.2-mm thick in the form of a cone of base diameter 4 mm and height 6.5 mm with a rounded tip surrounded by a flowing argon shield. The calculated adiabatic flame temperature was 2241 K. The burner was mounted on a carriage having accurate axial alignment and calibrated drive such that 0.1 mm along the flame axis corresponded to 1 cm on the X-axis of an XY-recorder.

The flame-ion mass spectrometer is shown in Fig. 1. The flame burned against a pinhole 0.1 mm in diameter in a platinum/iridium disc welded into a water-cooled stainless steel mounting. The sampling rate was about 1 atmospheric $cm^3\ s^{-1}$ (i.e. about 6% of the total premixed gas). A fast vapour booster pump (Edwards 9B4) maintained the first vacuum chamber near 10^{-4} torr. The ion beam was focussed electrostatically through a 2-mm orifice into a second vacuum chamber maintained below 5×10^{-6} torr by a six-inch diffusion pump (Edwards F603) and trap, where it was analysed by a 6-inch quadrupole mass filter of our own design operated by a commercially-available power supply (Extranuclear QPS 011-1). The mass-analysed ions can be detected with an off-axis electron multiplier (Bendix M306). In the present experiments, however, a simple parallel-plate Faraday cage was employed connected to a vibrating-reed electrometer (Cary 31) having a grid-leak resistance of 10^{11} ohms, and coupled to the Y-axis of the XY-recorder. Positive or negative ions may be detected by reversing the polarity on all

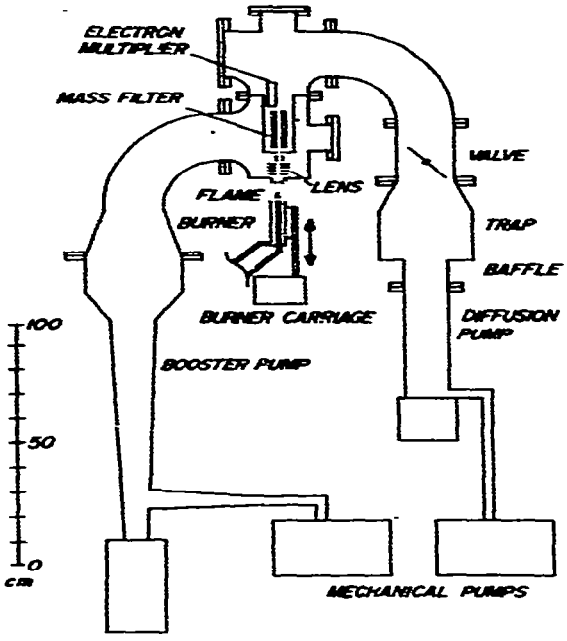

Fig. 1. Schematic diagram of the flame-ion mass spectrometer.

electrodes. Absolute calibration from measurement of the total ion current in the first chamber showed that approximately 20% of the ions entering the pinhole reached the mass filter.

Concurrent with the tracing of each ion profile, the flame pressure profile derived from an ionization gauge mounted in the second vacuum chamber was drawn on a second *XY*-recorder. The pressure profile showed a minimum corresponding to the downstream tip of the luminous reaction zone, and provided a reproducible origin ($z = 0$) in the flame for the distance scale of the ion profiles. The design of this flame-ion mass spectrometer was influenced by others [5,6]; one significant difference in this instrument is that the flame burns vertically upwards, thereby avoiding buoyancy effects when tracing axial profiles and enhancing stability.

RESULTS AND DISCUSSION

The ion chemistry is presumed to commence upstream with the accepted chemi-ionization reaction

$$CH + O \rightarrow CHO^+ + e \qquad \Delta H^\circ = -4 \qquad (1)$$

to form protonated CO and free electrons [7]. (Empirical formulae for ions

will be used throughout, but structural formulae for neutrals to avoid isomeric ambiguities. Standard enthalpies of reaction are quoted at room temperature in kcal mol^{-1}.) The very high concentration of O_2 assures the attachment of most of the electrons in a three-body process

$$e + O_2 + M \rightarrow O_2^- + M \qquad \Delta H^0 = -11.6 \qquad (2)$$

to form O_2^- ions. The CHO^+ and O_2^- primary ions are formed in a bath of neutral species with which they can react. The degree of ionization is sufficiently low (of order 1 in 10^8) so that the positive-ion and negative-ion chemistry can be considered to proceed independently, at least in the early stages of the flame.

What neutrals are available for reaction with the primary ions early in the reaction zone? Part of the answer is supplied by the beam sampling studies of Peeters and Mahnen [4] who obtained concentration profiles for a number of neutral species present in a flat methane–oxygen flame of fuel-lean composition ($\phi = 0.21$) at a pressure of 40 torr. Their profiles are shown in Fig. 2 where the distance scale z has been converted to atmospheric pressure assuming z inversely proportional to pressure. A new origin ($z = 0$)

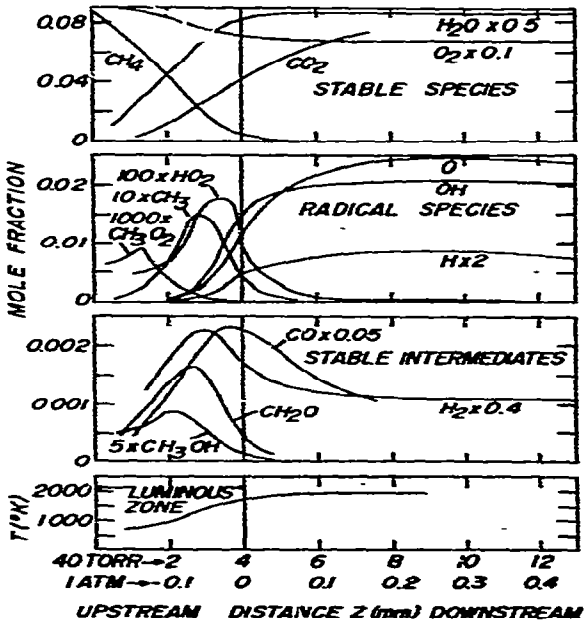

Fig. 2. Concentration profiles for neutral species observed by Peeters and Mahnen [4] in neutral beam sampling studies. Their measurements at $P = 40$ torr have been converted to atmospheric pressure by assuming distance $z \propto 1/P$.

based on the disappearance of methane has been included in conformity with our method described above. In the discussion of the flame-ion data to follow, evidence for these same neutrals will be considered, along with evidence for other neutrals not previously reported by these authors.

It will become apparent that the interpretation of individual profiles for both positive and negative ions is subject to the following general limitations.

1. More than one reaction channel may be involved in the production of a given ionic species.

2. A given ionic mass number may represent ions of different chemical composition or ions of different structure having the same chemical composition.

3. Isotopic species may account for a significant fraction of an ion profile.

4. The profile of an ion may be obscured by a cluster ion of the same mass number; for example, a hydrate.

These cases will be referred to by number when individual ion profiles are considered. A minor problem of purely instrumental origin arises because the peak shape inherent in quadrupole mass spectrometers is asymmetric towards low mass. It is therefore difficult to observe a small signal at mass M immediately preceding a very large signal at mass $(M + 1)$.

Positive ion chemistry

Primary CHO^+ ions formed early in the reaction zone will undergo proton transfer reactions with those neutral species present having a proton affinity (PA) higher than that of CO. Subsequent proton transfer reactions will favour those neutrals of progressively higher PA. A great many such reactions have been measured at room temperature [8] and are, in general, known to be fast ($k \simeq 10^{-9}$ cm^3 molecule^{-1} s^{-1}). The PA's of species which may be present early in the flame are given in Table 1 for room temperature and are, to our knowledge, the best values which have been measured to date. The values may be somewhat different at the higher temperature of the flame although the proton transfer reactions from which they are derived are not expected to be strongly temperature dependent; at least the relative order of the PA's should not vary significantly.

Selected positive ion profiles for fourteen mass numbers are given in Fig. 3 for a conical flame burning at atmospheric pressure having the same composition ($\phi = 0.215$) as that used for the neutral beam sampling studies of Peeters and Mahnen [4]. Since expansion cooling during sampling can enhance hydrate formation, the hydrate ion signals have been combined with that of the parent mass number where the contributions are appreciable and where the identity of the hydrate is not seriously in doubt; this treatment has been used by other workers [18]. Chemical assignments of these fourteen ionic mass numbers are given in Table 2, based on the addition of a proton to the corresponding neutral species.

In general, the observed ions are consistent with a reaction scheme early in

TABLE 1

Increasing proton affinities of neutral flame constituents

Atom or molecule	PA_{298} (kcal mol^{-1})	Reference	Atom or molecule	PA_{298} (kcal mol^{-1})	Reference
H_2	101.0 ± 1.2	[9]	C_2H_4	161 ± 3 [c]	[13,14]
O_2	101.5 ± 2.0 [a]	[10,11]	C_4H_2	162 ± 4 [c]	[14]
O	116.3 ± 0.9 [b]	[12]	H_2O	165 ± 3	[17]
CH_3	128 ± 2 [c]	[13,14]	HCHO	168 ± 1	[17]
CO_2	128.6 ± 1.3 [d]		HCOOH	175 ± 5	[17]
CH_4	130.9 ± 1.6 [d]		CH	176 ± 2 [c]	[13,14]
CO	142.6 ± 1.0	[12]	CH_3OH	182 ± 3	[17]
C_2H_6	144 ± 3 [d]		CH_3CHO	185 ± 2	[17]
OH	144 ± 2 [c]	[13,14]	C_2H_5OH	187 ± 2	[17]
C	149 ± 1 [c]	[13]	CH_3COOH	188 ± 3	[17]
HO_2	149 ± 7 [c]	[13,14]	CH_3OCH_3	190 ± 5	[17]
H_2O_2	151 ± $^{5}_{9}$ [e]	[15]	CH_2	200 ± 3 [c]	[13,14]
C_2H_2	153 ± 3 [c,f]	[13,16]	CH_2CO	201 ± 2	[17]
CHO	155 ± 4 [c]	[13,14]	CH_3COCH_3	202 ± 2	[17]

[a] Calculated using the equilibrium constant $K_{298} = 2.2 \pm 0.9$ for the reaction $H_3^+ + O_2 = HO_2^+ + H_2$.

[b] Calculated using the ionization potential $IP(OH) = 12.99$ V. See ref. [12] for the leading references.

[c] Calculated using standard heats of formation $\Delta H_{f,298}^{\circ}$ given in JANAF Tables [13] when available, or NSRDS-NBS 26 [14]. The latter reference does not quote uncertainties, which have been assumed to be ±2 kcal mol^{-1} for both ions and neutrals.

[d] From unpublished equilibrium constant measurements obtained using the York flowing afterglow apparatus.

[e] $PA(HO_2) < PA(H_2O_2) < PA(H_2O)$.

[f] Based on the appearance potential of $C_2H_3^+$ from C_2H_4 [16].

TABLE 2

Selected mass numbers and assignments of positive ions

Mass number (amu)	Empirical formula XH^+	Corresponding neutral X
13	CH^+	C
14	CH_2^+	CH
15	CH_3^+	CH_2
19 + 37 + 55 [a]	H_3O^+	H_2O
27	$C_2H_3^+$	C_2H_2
29	CHO^+ ($C_2H_5^+$)	CO (C_2H_4)
30	CH_2O^+	HCO
31 + 49	CH_3O^+ ($C_2H_7^+$)	HCHO (C_2H_6)
33 + 51 + 69	CH_5O^+	CH_3OH
43 + 61	$C_2H_3O^+$	CH_2CO
45 + 63	$C_2H_5O^+$	CH_3CHO
47 + 65	$CH_3O_2^+$ ($C_2H_7O^+$)	HCOOH (C_2H_5OH, CH_3OCH_3)
57 + 75	$C_3H_5O^+$	CH_3CHCO
59	$C_3H_7O^+$	C_2H_5CHO (CH_3COCH_3)

[a] Additional numbers given after the primary mass number are interpreted as representing successive hydrates which may be enhanced by expansion cooling during sampling. The corresponding profile shown in Fig. 3 is the sum of those observed at all of the mass numbers indicated.

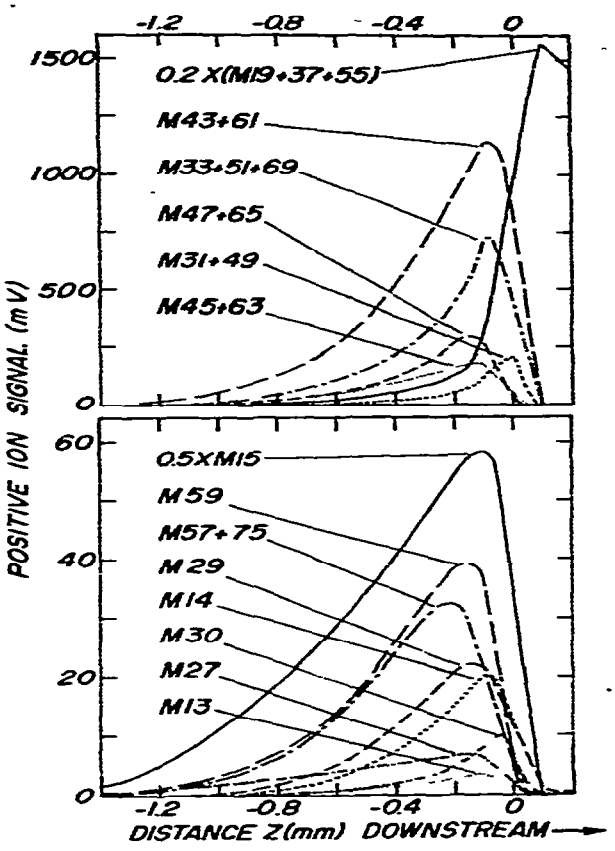

Fig. 3. Axial profiles of positive ions at selected mass numbers *M*. Additional numbers given after the primary mass number are interpreted as representing successive hydrates, and the profile shown is the sum of those observed at all of the mass numbers indicated.

the flame which is dominated by proton transfer processes. It is therefore convenient to discuss the profiles approximately in terms of increasing *PA* of the neutrals given in Table 1.

H_2, O_2, O, CH_3, CO_2, CH_4. The ions formed by protonating these neutrals which have *PA*'s less than that of CO should be absent, and indeed do not appear to be present. That is, ions of *M*3 * (H_3^+) and *M*17 (HO^+, CH_5^+) are not detected. A small signal at *M*16, which in fact persists far downstream, is attributed to O^+ rather than CH_4^+, and more logical candidates are discussed later for *M*33 and 45 than protonated O_2 and CO_2, respectively.

* *M*3, *M*17, etc. indicate mass numbers (*m*/*z*) 3, 17, etc.

C. The signal at *M*13 can only be CH^+ whose formation from CHO^+ is consistent with *PA* (C) > *PA* (CO) and may therefore indicate the presence of C atoms in the flame. The evidence is not conclusive, however, since reactions such as

$$CH_2^+ + OH \rightarrow CH^+ + H_2O \qquad \Delta H^0 = -11 \qquad (3)$$

may contribute to CH^+ formation (case 1).

OH, H_2O, HO_2, H_2O_2. While *M*18 corresponding to protonated OH can be detected, its profile (not shown in Fig. 3) is obscured by the very large H_3O^+ signal at *M*19. The upstream tail of the *M*19 profile (drawn 1/5 scale in Fig. 3) provides clear evidence for proton transfer to H_2O before other reactions take over to explain the rapid rise of the profile near $z = 0$ (case 1). No evidence was obtained for either HO_2 or H_2O_2 since isotopes account for all of the corresponding signals observed at *M*34 ($^{13}CH_5O^+$, CDH_4O^+, $CH_5{}^{17}O^+$) and *M*35 ($CH_5{}^{18}O^+$), respectively (case 3).

C_2H_2, C_2H_4, C_2H_6, C_4H_2. Appreciable concentrations of C_2- or C_4-hydrocarbons would not be expected in such a fuel-lean flame although they have been detected in a fuel-rich methane-oxygen flame [19]. The profile observed at *M*27 which must be $C_2H_3^+$ may involve direct protonation of C_2H_2, although other reactions are possible (case 1); for example

$$CH_x^+ + CH_y \rightarrow C_2H_3^+ + H \qquad (x + y) = 4 \qquad (4a)$$

$$\rightarrow C_2H_3^+ + H_2 \qquad (x + y) = 5 \qquad (4b)$$

The interpretation of the profiles at *M*29 and 31 is also somewhat ambiguous. Most of *M*29 is believed to be CHO^+ with a minor contribution from $C_2H_5^+$ arising from direct proton transfer to C_2H_4 or from reactions similar to eqn. (4) with $(x + y) = 6$ or 7. Mass 31 is believed to be mainly protonated formaldehyde CH_3O^+ rather than $C_2H_7^+$. In this instance, no counterpart to eqn. (4) is possible. The large signal measured at *M*51 (197 mV maximum, not shown separately in Fig. 3) is ascribed to the hydrate of *M*33 (case 4) which would obscure any minor contribution from protonated C_4H_2 even if the latter were present.

HCO, HCHO. The profile at *M*30 is ascribed to protonated HCO radicals; a rise of the profile further downstream (not shown in Fig. 3) is attributed to NO^+ as air is occluded through the argon shield. Reactions other than proton transfer might again contribute to the formation of CH_2O^+; for example

$$CH_2^+ + OH \rightarrow CH_2O^+ + H \qquad \Delta H^0 = -67 \qquad (5)$$

$$CH_3^+ + O \rightarrow CH_2O^+ + H \qquad \Delta H^0 = -44 \qquad (6)$$

The *M*31 profile provides strong evidence for HCHO, in agreement with the observations of Peeters and Mahnen [4].

HCOOH, C_2H_5OH, CH_3OCH_3. With regard to the *M*47 profile, the considerations of case 2 make HCOOH indistinguishable from the two structural isomers C_2H_5OH and CH_3OCH_3 which have higher *PA*'s.

CH, CH_2. Case 1 does not appear to apply to *M*14 since reactions such as

$$CH_3^+ + OH \rightarrow CH_2^+ + H_2O \qquad \Delta H^0 = 6 \tag{7}$$

are endothermic. If alternative production channels do not exist, the *M*14 profile is indicative of CH radicals.

The relatively large profile at *M*15 (drawn 1/2 scale in Fig. 3) is indicative of CH_2 radicals. The evidence for CH_2 is less ambiguous than that for C and CH. The counterpart of eqns. (3) and (7) should not occur since the formation upstream of CH_4^+ from CH_3 is unlikely, as pointed out previously.

CH_3OH, CH_3CHO, CH_3COOH. The profile at *M*33 is identified with CH_3OH in agreement with Peeters and Mahnen's result [4]. However they were apparently unable to detect CH_3CHO which must be responsible for the *M*45 profile if proton transfer reactions dominate; no other neutral appears to fit this mass number provided C_3H_8 and the unsaturated alcohol $CH_2 = CHOH$ are discounted. The identification of CH_3COOH at *M*61 is precluded by the hydrate of *M*43 (case 4).

CH_2CO, CH_3CHCO. The profile at *M*43 is thought to provide strong evidence for the presence of CH_2CO in the flame; the very large amplitude of the profile does not necessarily imply a high concentration of ketene but rather reflects its very high *PA*. Similarly, the profile at *M*57 appears to be protonated methyl ketene CH_3CHCO whose *PA* is not known but is expected to be comparable to that of ketene; other possible structures for neutral *M*56 (CH_2CHCHO and $HCCCH_2OH$) are less likely in view of the ketene evidence.

C_2H_5CHO, CH_3COCH_3. The profile at *M*59 provides evidence for either C_2H_5CHO or CH_3COCH_3 (case 2).

One final consideration is relevant to the discussion of positive ions; namely, the extent to which charge transfer can compete with proton transfer in the formation of a given ion. The HCO radical has the rather low ionization energy (*IE*) of 188 kcal mol^{-1} (or 8.15 eV) so that charge transfer reactions of CHO^+ with virtually all stable neutrals in the flame are endothermic. Few of the ions XH^+ formed as protonated neutrals are good reagents for charge transfer since the radical product XH will usually be unstable yielding X + H, making the overall reaction endothermic. Of possible importance are several neutral radicals having mass numbers identical with those of the ions of interest discussed above. Some of these have relatively low *IE*'s such as CH (*IE* = 246.8 kcal mol^{-1} or 10.70 eV), CH_2 (241 or 10.5), CH_3 (255 or 9.76) and CH_3O (≈167 or 7.24). Thus, the formation of the corresponding

ion for any one of these radicals, say CH_2^+, by charge transfer

$$CH^+ + CH_2 \rightarrow CH_2^+ + CH \qquad \Delta H^0 = -6 \tag{8}$$

may compete with its formation by proton transfer

$$CHO^+ + CH \rightarrow CH_2^+ + CO \qquad \Delta H^0 = -33 \tag{9}$$

For this example, the contribution of eqn. (8) to the profile at *M*14 is probably minor compared with that of proton transfer since a considerable number of flame ions can protonate CH.

In summary, the positive ion chemistry early in the reaction zone is qualitatively consistent with a simple proton transfer model initiated by primary CHO^+ ions. The flame-ion evidence for the neutral species present may be summarized as follows:

OH, H_2O, CO (C_2H_4), HCHO (C_2H_6), CH_3OH;

(b) species not reported by Peeters and Mahnen: C, C_2H_2, HCO, CH, CH_2, CH_3CHO, CH_2CO, CH_3CHCO;

(c) species not reported with chemical or isomeric ambiguities: HCOOH (C_2H_5OH, CH_3OCH_3), C_2H_5CHO (CH_3COCH_3).

Negative ion chemistry

The negative ion chemistry originates with O_2^- ions formed early in the reaction zone but is complicated by the fact that several types of reaction are possible. Charge transfer (*CT*) of electrons will have a trend in favour of those neutrals present of increasingly high electron affinity (*EA*). The *EA*'s of a number of species which may be present early in the flame are given in Table 3 in order of increasing *EA*. Secondly, proton transfer (*PT*) reactions are possible for those negative ions present of sufficiently high base strength to abstract protons from neutral "acids". The *PA*'s of a number of negative ions are given in Table 4 for room temperature in order of decreasing base strength; a given negative ion is energetically capable of proton abstraction from the corresponding neutral (conjugate acid) of a lower member of Table 4. Thirdly, O_3^- and other negative ions may undergo rearrangement reactions with some neutrals in processes other than *CT* or *PT* (designated *R* for rearrangement). Finally, negative ions including O_2^- may take part in three-body association reactions to form cluster ions (designated *C* for clustering); for example, the clustering of O_2^- with O_2 to form O_4^-. In some cases, these cluster ions may subsequently undergo fast switching reactions in which the neutral clustered to the ion is replaced by a different neutral (designated *S* for switching). In all cases, the negative product ion will not necessarily be detectable if it reacts rapidly with O_2 or CH_4.

Little information is presently available for the rate constants of charge transfer reactions of O_2^-, particularly with flame radicals, most of which have

TABLE 3

Increasing electron affinities of flame constituents

Atom or molecule	EA_0^0 (kcal mol^{-1})	EA_0^0 (eV molecule^{-1})	$\Delta H^0_{f,298}$ (neg. ion)[a] (kcal mol^{-1})	Reference
CH_2	4.8 ± 0.7	0.21 ± 0.03	86 ± 2	[13,20]
O_2	10.1 ± 0.2	0.440 ± 0.008	−11.6 ± 0.2	[21]
H	17.392	0.75421	33.231 ± 0.001	[13,22]
CH	28.55 ± 0.18	1.238 ± 0.008	112.0 ± 0.3	[13,23]
C	29.24 ± 0.12	1.268 ± 0.005	140.2 ± 0.6	[13,22]
O	33.71 ± 0.07	1.462 ± 0.003	24.4 ± 0.1	[13,22]
CH_3O	<36.7 ± 0.9	<1.59 ± 0.04	>(−34 ± 2)	[24,25]
C_2H_5O	<39 ± 4[b]	<1.7 ± 0.2	>(−46 ± 3)	[25]
CHCO	>41 ± 4[b]	>1.8 ± 0.2	<(−6 ± 3)	[26]
OH	42.09 ± 0.05	1.825 ± 0.002	−34.1 ± 0.1	[13,27]
O_3	48 ± 2	2.1 ± 0.1	−15 ± 2	[13,28]
HO_2	~69	~3.0	~−66	[13,29]
HCO_2	~77	~3.3	~118	[30]
C_2	<81.7	<3.54	>117	[13,31]
C_2H	<86.0,<62 ± 4[b]	<3.73,<2.7 ± 0.2	>41 ± 1,>64 ± 3	[13,31,32]

[a] The standard heat of formation at 298K for a negative ion Y^- is calculated from the expression $\Delta H^\circ_{f,298}(Y^-) \cong \Delta H^\circ_{f,298}(Y) - EA_0^0(Y) - 1.480$ kcal mol^{-1}, where the last term represents (5/2) RT for the electron with $R = 1.987$ cal mol^{-1} deg^{-1} and $T = 298$ K.
[b] Based on unpublished results from the York flowing afterglow apparatus.

TABLE 4

Proton affinities of negative flame ions in order of decreasing base strength

Negative ion	PA_{298} (kcal mol^{-1})	Reference
CH_2^-	418 ± 2[a]	[13]
H^-	400.42 ± 0.01[a]	[13]
CH_3^-, $C_2H_3^-$, $C_2H_5^-$	>400[b]	
OH^-	390.9 ± 0.1[a]	[13]
CH^-	387 ± 1[a]	[13]
O^-	382.1 ± 0.2[a]	[13]
CH_3O^-	381 ± 2[c]	[13,14]
C_2HO^-	<380 ± 6[b,c]	[13,14]
$C_2H_5O^-$	>377 ± 5[b,c]	[13,14]
C_2^-	>370[a]	[13]
C^-	365.4 ± 0.7[a]	[13]
$C_2H_3O_2^-$	~360	[13,14]
C_2H^-	>354 ± 1, <375 ± 4[b,c]	[13]
O_2^-	351 ± 2[a]	[13]
CHO_2^-	~344	[13,14]
HO_2^-	~334[a]	[13]

[a] Calculated using $\Delta H^\circ_{f,298}$ (negative ion) values from Table 3 and standard heats of formation at 298K from JANAF Tables [13] and NSRDS-NBS 26 [14]. Where the latter reference has been used, the only significant contribution to the uncertainties is that for ketene where $\Delta H^\circ_{f,298}(CH_2CO) = -14.6 \pm 1$ kcal mol^{-1} has been assumed.
[b] Based on unpublished results from the York flowing afterglow apparatus.
[c] Based on $EA^\circ_0(CH_3O) = 36.7 \pm 0.9$ or $\Delta H^\circ_{f,298}(CH_3O^-) = -34 \pm 2$ kcal mol^{-1}.

EA's higher than that of O_2^- (Table 3). In contrast, the low base strength of O_2^- will render many of its proton transfer reactions endothermic (Table 4). The O_2^- ion will undergo associative detachment reactions with several small flame neutrals (e.g. H and O) at room temperature [33]. However, not much is known about O_2^- rearrangement reactions, particularly above room temperature in the flame where rearrangement may successfully compete with associative detachment. The kinetics of clustering involving O_2^- and subsequent switching reactions are well established at room temperature [34]. The former are expected to exhibit a negative temperature dependence while the latter should be relatively temperature independent.

Selected negative ion profiles of thirteen mass numbers are given in Fig. 4 for the same fuel-lean flame specified above; the treatment of hydrates is the

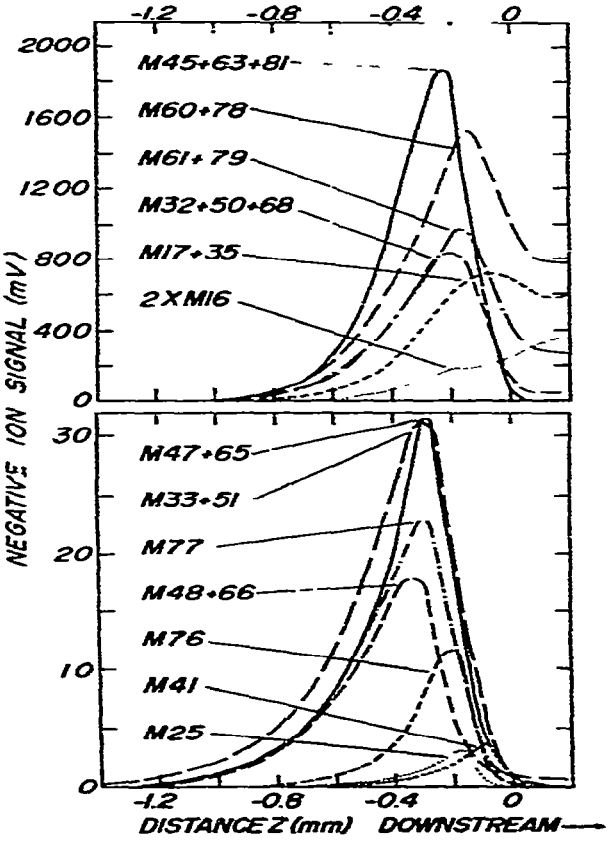

Fig. 4. Axial profiles of negative ions at selected mass numbers *M*. Additional numbers given after the primary mass number are interpreted as representing successive hydrates, and the profile shown is the sum of those observed at all of the mass numbers indicated.

TABLE 5

Selected mass numbers and assignments of negative ions

Mass number (amu)	Empirical formula	Related neutral [b]
16	O^-	OH (*PT*); O (*CT*)
17 + 35 [a]	OH^-	OH (*CT*)
25	C_2H^-	C_2H_2 (*PT*); C_2H (*CT*)
32 + 50 + 68	O_2^-	O_2 (by 3-body electron attachment)
33 + 51	HO_2^-	HO_2 (*CT*); H_2O_2 (*PT*)
41	C_2HO^-	CH_2CO (*PT*); CHCO (*CT*)
45 + 63 + 81	CHO_2^- ($C_2H_5O^-$)	HCOOH (C_2H_5OH, CH_3OCH_3) (*PT*); HCO_2 (*CT*); HCHO (*R*)
47 + 65	$CH_3O_2^-$	CH_3O_2 (*CT*)
48 + 66	O_3^-	O_3 (*CT*); O (*R*)
60 + 78	CO_3^-	CO_2 (*R*, *C*); CO (*S*)
61 + 79	CHO_3^-	CO_2 (*C*); CO (*S*)
76	CO_4^-	CO_2 (*C*, *S*)
77	CHO_4^-	CO_2 (*C*, *S*)

[a] Additional numbers given after the primary mass number are interpreted as representing successive hydrates which may be enhanced by expansion cooling during sampling. The corresponding profile shown in Fig. 4 is the sum of those observed at all the mass numbers indicated.

[b] Formation of the ion from the related neutral may involve change transfer (*CT*), proton transfer (*PT*), rearrangement (*R*) and clustering (*C*); the cluster ions may also take part in switching reactions (*S*).

same as that for positive ions. Assignments of these negative ions are given in Table 5 together with the neutrals involved in their production by *CT*, *PT*, *R*, *C* and *S* reactions. The negative ions will be discussed in groups where similar considerations are involved in order to evaluate the evidence for neutral species present early in the flame. Initially at least, the discussion approximately follows the ion order of Table 4.

H^-, CH_2^-, CH_3^-. None of these ions was detected in this flame. Only H^- would be formed by charge transfer of the corresponding neutral radical with O_2^-. *EA* (CH_3), although not well established [35], is expected to be lower than *EA* (O_2). Furthermore, the low acidity of H_2, CH_3 and CH_4 precludes the formation of the corresponding anions by proton transfer; that is, these anions are very strong bases (see Table 4). The H^- formed by charge transfer to H would be expected to disappear in rapid proton transfer reactions with a variety of neutral species in the flame, or by associative detachment; for example

$$H^- + O_2 \rightarrow HO_2 + e \qquad \Delta H^0 = -28 \qquad (10)$$

for which $k_{10} = 1.2 \times 10^{-9}$ cm^3 molecule^{-1} s^{-1} at 300 K [33].

$C_2H_3^-$, $C_2H_5^-$. Both these ions were also not detected. The energetics for their formation by charge or proton transfer are again unfavourable. These ions

would therefore be unsuitable for the *CI* detection of C_2H_3 and C_2H_5 (*CT*) or C_2H_4 and C_2H_6 (*PT*).

OH^-. The failure to observe those negative ions listed above which are sufficiently strong bases to abstract protons from water suggests that proton transfer is not a major source of the OH^- observed early in the flame. One possible source is charge transfer

$$O_2^- + OH \rightarrow OH^- + O_2 \qquad \Delta H^0 = -32.0 \qquad (11)$$

in which case the OH^- profile would be indicative of the growth of OH radicals in the flame. Alternatively OH^- may be formed by the H-atom transfer reaction of O^- with CH_4

$$O^- + CH_4 \rightarrow OH^- + CH_3 \qquad \Delta H^0 = -5.8 \qquad (12)$$

for which $k_{12} = 1.0 \times 10^{-10}$ cm^3 molecule^{-1} s^{-1} at 300 K [36], or with other hydrocarbons. Consequently the OH^- ion profile does not provide evidence for any single neutral species.

C^-, CH^-. Although neither was observed, both ions could be formed by charge transfer from O_2^- to C and CH, or by proton transfer from CH and CH_2 to a sufficiently strong base (e.g. OH^-). However, the ions may be lost in rearrangement reactions with O_2

$$C^- + O_2 \rightarrow O^- + CO \qquad \Delta H^0 = -142.2 \qquad (13)$$

$$CH^- + O_2 \rightarrow OH^- + CO \qquad \Delta H^0 = -172.5 \qquad (14a)$$

$$\rightarrow O^- + HCO \qquad \Delta H^0 = -77.2 \qquad (14b)$$

where $k_{13} = 4.0 \times 10^{-10}$ cm^3 molecule^{-1} s^{-1} at 300 K [37], or possibly by associative detachment

$$C^- + O \rightarrow CO + e \qquad \Delta H^0 = -226.2 \qquad (15)$$

$$CH^- + OH \rightarrow HCHO + e \qquad \Delta H^0 = -149.2 \qquad (16)$$

The absence of detectable C^- and CH^- fails to corroborate the positive ion evidence for the presence of any of the CH_x ($x = 0 - 2$) radicals.

O^-. Although associative detachment,

$$O_2^- + O \rightarrow O_3 + e \qquad \Delta H^0 = -13.9 \qquad (17)$$

for which $K_{17} \sim 2 \times 10^{-10}$ cm^3 molecule^{-1} s^{-1} at 300 K [33], is dominant near room temperature, charge transfer

$$O_2^- + O \rightarrow O^- + O_2 \qquad \Delta H^0 = -23.6 \qquad (18)$$

may become predominant as the temperature increases through the reaction zone. Similar considerations may apply to the production of O^- by proton

abstraction from OH by the stronger bases in Table 4 such as

$$OH^- + OH \rightarrow O^- + H_2O \qquad \Delta H^0 = -8.8 \qquad (19)$$

since, once again, associative detachment

$$OH^- + OH \rightarrow H_2O_2 + e \qquad \Delta H^0 = -8.0 \qquad (20)$$

may dominate near room temperature. Even when formed, O^- can react directly with CH_4 by eqn. (12). These two factors may explain the late rise of the O^- profile at a point in the reaction zone where CH_4 is somewhat depleted, and the increased temperature probably mitigates against associative detachment processes whose rate coefficients, in general, have been observed to decrease with increasing ion kinetic energy [33]. Overall, the O^- profile must provide evidence for either O or OH, but the two cannot be distinguished.

CH_3O^-. No ion was detected at *M*31, perhaps partly because it immediately precedes the large O_2^- signal observed at *M*32. The moderate electron affinity of CH_3O and moderate acidity of CH_3OH would favour the formation of CH_3O^- early in the flame once O_2^-, O^- or OH^- have become established. However, the possible subsequent reaction of CH_3O^- with O_2

$$CH_3O^- + O_2 \rightarrow CHO_2^- + H_2O \qquad \Delta H^0 \leqslant -138 \qquad (21a)$$

$$\rightarrow HO_2^- + HCHO \qquad \Delta H^0 \leqslant -60 \qquad (21b)$$

would render the observation of this ion difficult.

C_2H^-, *HO_2^-*, *C_2HO^-*. These three ions each pose a similar dilemma. For example, HO_2^- may arise either by proton transfer from H_2O_2

$$OH^- + H_2O_2 \rightarrow HO_2^- + H_2O \qquad \Delta H^0 = -57 \qquad (22)$$

or by charge transfer to HO_2 radicals

$$O_2^- + HO_2 \rightarrow HO_2^- + O_2 \qquad \Delta H^0 = -59 \qquad (23)$$

The HO_2^- profile is the earliest measured upstream. The same dilemma applies to the pairs C_2H_2/C_2H and $CH_2CO/CHCO$. Other reactions may further complicate this situation; several channels have been measured in the approximate proportions shown for the reaction of O^- with C_2H_2 at room temperature [38]

$$O^- + C_2H_2 \xrightarrow{0.6} CH_2CO + e \qquad \Delta H^0 = -93.2 \qquad (24a)$$

$$\xrightarrow{0.3} C_2H^- + OH \qquad \Delta H^0 \geqslant (-28), \leqslant (-7) \qquad (24b)$$

$$\xrightarrow{0.05} C_2HO^- + H \qquad \Delta H^0 \leqslant (-28) \qquad (24c)$$

$$\xrightarrow{0.05} C_2^- + H_2O \qquad \Delta H^0 \geqslant (-19) \qquad (24d)$$

In neutral beam sampling studies of a fuel-rich methane—oxygen flame by Hastie [19], C_2H_2 but not C_2H was detected, and the $M25$ profile is therefore taken as evidence for acetylene in the present case. Conversely, the profile at $M33$ as HO_2^- produced by charge transfer from O_2^- would confirm the presence of HO_2 radicals reported by Peeters and Mahnen [4]. Our positive ion evidence at $M43$ for the presence of CH_2CO indicates that the negative $M41$ profile can be attributed to proton abstraction from ketene, probably by OH^- and O^-. It should be noted that the $M43^+$ and $M41^-$ profiles maximize at the same position in the flame. For the three ions C_2H^-, HO_2^- and C_2HO^-, however, no single consistent mechanism appears to be operative.

CHO_2^-. The profile at $M45$ yields the largest negative ion signals measured, and many sources can be envisaged. The CHO_2^- ion could be produced either by proton transfer involving virtually all the ions in Table 4 including O_2^-

$$O_2^- + HCOOH \rightarrow CHO_2^- + HO_2 \qquad \Delta H^0 = -7 \tag{25}$$

since in this case O_2^- is a stronger base than CHO_2^-, or by charge transfer to the HCO_2 radical

$$O_2^- + HCO_2 \rightarrow CHO_2^- + O_2 \qquad \Delta H^0 = -63.2 \tag{26}$$

A considerable number of rearrangement reactions with flame neutrals could lead to CHO_2^- such as

$$O_2^- + CH_3 \rightarrow CHO_2^- + H_2 \qquad \Delta H^0 = -137 \tag{27}$$

$$O_2^- + CH_2CO \rightarrow CHO_2^- + CHO \qquad \Delta H^0 = -77 \tag{28}$$

$$O^- + HCHO \rightarrow CHO_2^- + H \qquad \Delta H^0 = -59 \tag{29a}$$

$$\rightarrow OH^- + CHO \qquad \Delta H^0 = -20 \tag{29b}$$

where $k_{29} = 3.1 \times 10^{-9}$ cm^3 molecule^{-1} s^{-1} at 300 K [39], which are energetically and chemically reasonable. A number of these reactions are presently under investigation in our flowing afterglow laboratory. Also, proton abstraction from C_2H_5OH or CH_3OCH_3 will yield the same mass number (case 2 above). The possibilities are too numerous to provide clear evidence for any single neutral species. It is likely that many of these reactions may, in fact, contribute to the negative $M45$ profile.

$CH_3O_2^-$, O_3^-. The $M47$ profile is the second earliest measured upstream. Although some part of the profile shown in Fig. 4 derives from an isotopic contribution from $M45$ ($CH^{18}O^{16}O^-$, case 3 above) and a hydrate contribution, the peak positions of the two profiles are significantly different. No neutral exists at $M48$ to provide a logical proton transfer possibility. Thus, $M47$ appears to derive from charge transfer

$$O_2^- + CH_3O_2 \rightarrow CH_3O_2^- + O_2 \tag{30}$$

involving the same radical species detected far upstream by Peeters and Mahnen [4].

Similarly, the $M48$ profile has an early upstream tail and, presumably, a large hydrate contribution. No reasonable possibility exists for its production by proton transfer. It can be formed by charge transfer

$$O_2^- + O_3 \rightarrow O_3^- + O_2 \qquad \Delta H^0 = -38 \tag{31}$$

$$O^- + O_3 \rightarrow O_3^- + O \qquad \Delta H^0 = -14 \tag{32}$$

for which $k_{31} = 3.0 \times 10^{-10}$ [40] and $k_{32} = 5.3 \times 10^{-10}$ cm^3 molecule^{-1} s^{-1} [41] at 300 K, although a rearrangement reaction has been measured at room temperature

$$O_4^- + O \rightarrow O_3^- + O_2 \tag{33a}$$

$$\rightarrow O^- + 2O_2 \tag{33b}$$

for which $k_{33} = 4.0 \times 10^{-10}$ cm^3 molecule^{-1} s^{-1} at 300 K [42]. Nevertheless, O_3^- is thought to provide evidence for the presence of ozone in the flame.

CO_3^-, CHO_3^-, CO_4^-, CHO_4^-. It is well known from flowing afterglow studies of ionospheric chemistry that these ions are highly stable [42]. It is therefore not surprising that many modes can be envisaged for their production. Some likely two-body flame reactions might be

$$O_3^- + CO_2 \rightarrow CO_3^- + O_2 \tag{34}$$

$$CO_3^- + HX \rightarrow CHO_3^- + X \tag{35}$$

$$O_4^- + CO_2 \rightarrow CO_4^- + O_2 \tag{36}$$

$$CO_4^- + HX \rightarrow CHO_4^- + X \tag{37}$$

for which $k_{34} = 4.0 \times 10^{-10}$ [40] and $k_{36} = 4.3 \times 10^{-10}$ cm^3 molecule^{-1} s^{-1} [34] at 300 K, where HX is an H-atom donor. Some three-body clustering reactions (C) which may contribute to the formation of these ions include

$$O^- + CO_2 + M \rightarrow CO_3^- + M \tag{38}$$

$$OH^- + CO_2 + M \rightarrow CHO_3^- + M \tag{39}$$

$$O_2^- + CO_2 + M \rightarrow CO_4^- + M \tag{40}$$

$$HO_2^- + CO_2 + M \rightarrow CHO_4^- + M \tag{41}$$

Alternatively, these ions may be formed indirectly by three-body association followed by switching reactions

$$O_2^- \cdot H_2O + CO \rightarrow CO_3^- + H_2O \tag{42}$$

$$HO_2^- \cdot H_2O + CO \rightarrow CHO_3^- + H_2O \tag{43}$$

$$O_2^- \cdot H_2O + CO_2 \rightarrow CO_4^- + H_2O \quad (44)$$

$$HO_2^- \cdot H_2O + CO_2 \rightarrow CHO_4^- + H_2O \quad (45)$$

The degree to which these latter eight reactions also occur during sampling is uncertain. In any event, these four ions CO_3^-, CHO_3^-, CO_4^-, CHO_4^- present some evidence for CO_2 and CO, albeit in a complicated manner.

In summary, the negative ion chemistry initiated by O_2^- is quite complex and cannot be described by a simple model since a large variety of reaction types appear to be involved. The flame-ion evidence for the neutral species may be summarized as follows:

(a) species which corroborate the observations of Peeters and Mahnen: O_2, H_2O, O, OH, HO_2 (or H_2O_2), HCHO, CH_3O_2, CO, CO_2;

(b) new species not reported by Peeters and Mahnen: C_2H_2 (or C_2H), CH_2CO (or CHCO), O_3;

(c) species not reported with chemical or isomeric ambiguities: HCOOH (or HCO_2); (C_2H_5OH, CH_3OCH_3).

CONCLUSIONS

The purpose of this work was to ascertain what can be learned from ion profiles concerning the neutral species present early in a flame viewed as a site for in situ chemical ionization. The degree to which the early ion profile shape can be related to the growth of a neutral species is determined by the degree of confidence one has in ascertaining the dominant ion chemistry. The recent rapid growth of information about individual ion—molecule reactions has made possible the realization of a model which provides a reasonable description of the inherently-complex flame-ion chemistry. The model views the positive and negative ion chemistry as proceeding independently in the early stages of combustion. This allows, at least in principle, two independent means of identification of a given neutral by chemical ionization, albeit not often realized in this study. Perhaps more significant is the potentially increased range of neutrals that can be distinguished.

The major primary ions CHO^+ and O_2^- are not seriously in doubt. Early in the flame, the positive ion chemistry is dominated by fast proton transfer reactions. The protons initially available from CHO^+ shuffle amongst the neutral species present with a trend towards those of high proton affinity; a large ion signal reflects a high proton affinity and/or high concentration of the neutral. The behaviour at the higher temperatures of the flame is qualitatively predictable from room-temperature measurements of rate constants for proton transfer reactions which are not, in general, strongly temperature dependent. Charge transfer does not appear to compete seriously with proton transfer early in the flame.

The negative ion chemistry is much more complicated since a variety of chemical ionization processes may operate. Very early in the flame, the mechanism appears to be charge transfer from the primary O_2^- ion to radicals

(and ozone) having higher EA's than O_2. This establishes appreciable concentrations of ions having a high base strength (e.g. OH^-, O^-), so that the proton transfer mechanism becomes competitive. Alternatively, O_2^- may undergo direct proton transfer with a few flame neutrals (e.g. HCOOH) although O_2^- is itself a very weak base. The competition of charge and proton transfer creates a dilemma since many of the observed anions R^- may derive either from charge transfer to the neutral radical R or from proton abstraction from the parent neutral RH. Furthermore, additional complications arise from rearrangement reactions leading to R^- as well as secondary reactions of R^- with the O_2/CH_4 bath. Still other reactions can contribute significantly to the formation of ions of high mass (e.g. CO_3^-, CHO_3^-, CO_4^-, CHO_4^-), namely, three-body association to form cluster ions which may subsequently undergo switching reactions. The degree to which sampling may play a role in this connection has not yet been determined. Despite these complications, negative chemical ionization provides additional and complementary evidence to the positive ion results.

ACKNOWLEDGEMENTS

This work was supported by the National Research Council of Canada.

REFERENCES

1 B. Munson, Anal. Chem. A, 43 (1971) 28.
2 H.I. Schiff and D.K. Bohme, Int. J. Mass Spectrom. Ion Phys., 16 (1975) 167.
3 J.L. Franklin (Ed.), Ion—Molecule Reactions, Vols. 1 and 2, Plenum Press, New York, 1972.
4 J. Peeters and G. Mahnen, Fourteenth Symposium (International) on Combustion, The Combustion Institute, Pittsburgh, Penna., 1973, p. 133.
5 A.N. Hayhurst, F.R.G. Mitchell and N.R. Telford, Int. J. Mass Spectrom. Ion Phys. 7 (1971) 177.
6 A.N. Hayhurst and T.M. Sugden, Proc. Roy. Soc. (London), Ser. A, 293 (1966) 36.
7 H.F. Calcote, Eighth Symposium (International) on Combustion, Williams and Wilkins, Pittsburgh, Penna., 1962, p. 184.
8 D.K. Bohme, in P. Ausloos (Ed.), Interactions Between Ions and Molecules, Plenum Press, New York, 1975, p. 489.
9 A.J. Duben and J.P. Lowe, J. Chem. Phys., 55 (1971) 4270.
10 F.C. Fehsenfeld, W. Lindinger and D.L. Albritton, J. Chem. Phys., 63 (1975) 443.
11 J.K. Kim, L.P. Theard and W.T. Huntress Jr., Chem. Phys. Lett., 32 (1975) 610.
12 P.M. Guyon, W.A. Chupka and J. Berkowitz, J. Chem. Phys., 64 (1976) 1419.
13 a) D.R. Stull and H. Prophet et al., JANAF Thermochemical Tables, 2nd Ed., NSRDS-NBS 37, U.S. Government Printing Office, 1971; b) M.W. Chase, J.L. Curnutt, A.T. Hu, H. Prophet, A.N. Syverud and L.C. Walker, JANAF Thermochemical Tables, 1974 Suppl., J. Phys. Chem. Ref. Data, 3 (1974) 311; c) M.W. Chase, J.L. Curnutt, H. Prophet, R.A. McDonald and A.N. Syverud, JANAF Thermochemical Tables. 1975 Suppl., J. Phys. Chem. Ref. Data, 4 (1975) 1.
14 J.L. Franklin, J.G. Dillard, H.M. Rosenstock, J.T. Herron, K. Draxl and T.H. Field, Ionization Potentials, Appearance Potentials, and Heats of Formation of Gaseous Positive Ions, NSRDS-NBS 26, U.S. Government Printing Office, 1969.

15 W. Lindinger, D.L. Albritton, C.J. Howard, F.C. Fehsenfeld and E.E. Ferguson, J. Chem. Phys., 63 (1975) 5220.
16 W.A. Chupka, J. Berkowitz and K.M.A. Refaey, J. Chem. Phys., 50 (1969) 1938.
17 J. Long and B. Munson, J. Am. Chem. Soc., 95 (1973) 2427.
18 A.N. Hayhurst and N.R. Telford, J. Chem. Soc., Faraday Trans. I, 70 (1974) 1999.
19 J.W. Hastie, Combust. Flame, 21 (1973) 187.
20 P.T. Zittel, G.B. Ellison, S.V. O'Neil, E. Herbst, W.C. Lineberger and W.P. Reinhardt, J. Am. Chem. Soc., 98 (1976) 3731.
21 R.J. Celotta, R.A. Bennett, J.L. Hall, M.W. Siegel and J. Levine, Phys. Rev. A, 6 (1972) 631.
22 H. Hotop and W.C. Lineberger, Binding Energies in Atomic Negative Ions, J. Phys. Chem. Ref. Data, 4 (1975) 539.
23 A. Kasdan, E. Herbst and W.C. Lineberger, Chem. Phys. Lett., 31 (1975) 78.
24 K.J. Reed and J.I. Brauman, J. Am. Chem. Soc., 97 (1975) 1625.
25 S.W. Benson, Thermochemical Kinetics, John Wiley & Sons, Inc., New York, 1968.
26 J.E. Collin and R. Locht, Int. J. Mass Spectrom. Ion Phys., 3 (1970) 465.
27 H. Hotop, T.A. Patterson and W.C. Lineberger, J. Chem. Phys., 60 (1974) 1806.
28 R. Byerly and E.C. Beaty, J. Geophys. Res., 76 (1971) 4596.
29 H.O. Pritchard, Chem. Rev., 52 (1953) 529.
30 Y. Yamdagni and P. Kebarle, J. Am. Chem. Soc., 95 (1973) 4050.
31 D. Feldman, Z. Naturforsch. A, 25 (1970) 621.
32 H. Okabe and V.H. Dibeler, J. Chem. Phys., 59 (1973) 2430.
33 F.C. Fehsenfeld, in P. Ausloos (Ed.), Interactions Between Ions and Molecules, Plenum Press, New York, 1975.
34 N.G. Adams, D.K. Bohme, D.B. Dunkin, F.C. Fehsenfeld and E.E. Ferguson, J. Chem. Phys., 52 (1970) 3133.
35 K.J. Reed and J.I. Brauman, J. Chem. Phys., 61 (1974) 4830.
36 D.K. Bohme and F.C. Fehsenfeld, Can. J. Chem., 47 (1969) 2717.
37 F.C. Fehsenfeld and E.E. Ferguson, J. Chem. Phys., 53 (1970) 2614.
38 D.K. Bohme, G.I. Mackay, H.I. Schiff and R.S. Hemsworth, J. Chem. Phys., 61 (1974) 2175.
39 Unpublished result from the York flowing afterglow laboratory.
40 F.C. Fehsenfeld, A.L. Schmeltekopf, H.I. Schiff and E.E. Ferguson, Planet. Space Sci., 15 (1967) 373.
41 E.E. Ferguson, F.C. Fehsenfeld and A.L. Schmeltekopf, Adv. Chem. Ser., 80 (1969) 83.
42 F.C. Fehsenfeld, E.E. Ferguson and D.K. Bohme, Planet. Space Sci., 17 (1969) 1759.